RESEARCH   **Open Access**

Long non-coding ribonucleic acid SNHG18 induced human granulosa cell apoptosis via disruption of glycolysis in ovarian aging

Xuehan Zhao[1,3†], Feiyan Zhao[2†], Long Yan[3,4,5,6], Jiaqi Wu[1,3], Ying Fang[1], Cong Wang[1], Zhimin Xin[1*] and Xiaokui Yang[1*]

Abstract

Background In-depth understanding of dynamic expression profiles of human granulosa cells (GCs) during follicular development will contribute to the diagnostic and targeted interventions for female infertility. However, genome-scale analysis of long non-coding ribonucleic acid (lncRNA) in GCs across diverse developmental stages is challenging. Meanwhile, further research is needed to determine how aberrant lncRNA expression participates in ovarian diseases.

Methods Granulosa cell-related lncRNAs data spanning five follicular development stages were retrieved and filtered from the NCBI dataset (GSE107746). Stage-specific lncRNA expression patterns and mRNA-lncRNA co-expression networks were identified with bioinformatic approaches. Subsequently, the expression pattern of *SNHG18* was detected in GCs during ovarian aging. And *SNHG18* siRNA or overexpression plasmids were transfected to SVOG cells in examining the regulatory roles of *SNHG18* in GC proliferation and apoptosis. Moreover, whether PKCε/SNHG18 signaling take part in GC glycolysis via ENO1 were verified in SVOG cells.

Results We demonstrated that GC-related lncRNAs were specifically expressed across different developmental stages, and coordinated crucial biological functions like mitotic cell cycle and metabolic processes in the folliculogenesis. Thereafter, we noticed a strong correlation of *PRKCE* and *SNHG18* expression in our analysis. With downregulated *SNHG18* of GCs identified in the context of ovarian aging, *SNHG18* knockdown could further induce cell apoptosis, retard cell proliferation and exacerbate DNA damage in SVOG cell. Moreover, downregulated PKCε/SNHG18 pathway interrupted the SVOG cell glycolysis by lowering the ENO1 expression.

Conclusions Altogether, our results revealed that folliculogenesis-related lncRNA *SNHG18* participated in the pathogenesis of ovarian aging, which may provide novel biomarkers for ovarian function and new insights for the infertility treatment.

Keywords Granulosa cell, Follicular development, lncRNA, Transcriptomics, *SNHG18*, Ovarian aging, Glycolysis

†Xuehan Zhao and Feiyan Zhao contributed equally to this work and share first authorship.

*Correspondence:
Zhimin Xin
xinzhimin@ccmu.edu.cn
Xiaokui Yang
yangxiaokui@ccmu.edu.cn
[1]Department of Human Reproductive Medicine, Beijing Obstetrics and Gynecology Hospital, Beijing Maternal and Child Health Care Hospital, Capital Medical University, Beijing 100026, China

[2]Department of Obstetrics and Gynecology, Beijing Chao-Yang Hospital, Capital Medical University, Beijing 100020, China
[3]Key Laboratory of Organ Regeneration and Reconstruction, State Key Laboratory of Stem Cell and Reproductive Biology, Institute of Zoology, Chinese Academy of Sciences, Beijing 100101, China
[4]Institute for Stem Cell and Regeneration, Chinese Academy of Sciences, Beijing 100101, China
[5]University of Chinese Academy of Sciences, Beijing 100049, China
[6]Beijing Institute for Stem Cell and Regenerative Medicine, Beijing 100101, China

Zhao *et al. Journal of Ovarian Research*   (2024) 17:185

Page 2 of 17

Background

Ovaries, being considered as the main reproductive organs, sustain female fertility by discharging oocytes and safeguard life quality through sex hormone biosynthesis. As the core functional unit of ovary, follicles constantly progress to developmental stages throughout the female reproductive lifespan, during which primordial follicles sequentially develop into primary, secondary, antral, and preovulatory follicles [1]. Compelling evidence has indicated that folliculogenesis relies on the interactions of oocyte and somatic cells, particularly with surrounding granulosa cells (GCs) [2, 3]. The granulosa cells will proliferate and differentiate into cumulus cells and mural granulosa cells after the recruitment of the primordial follicle, determining the oocyte developmental potential through transmission of metabolites [2, 4], paracrine signals [5, 6] and RNAs [7, 8]. As reported, a considerable number of molecules are involved in the regulation of GC proliferation and apoptosis [9, 10], as well as the ability of cumulus cells to generates ATP needed for oocyte meiotic resumption and maturation [4, 11, 12]. GC dysfunction is supposed to be one of the important causes of follicular atresia, thereby participating in the pathogenesis of ovarian aging [13–16]. Despite the GCs should transcribe differently at different developmental stages to exert diverse biological functions and meet the metabolic needs of follicles [17, 18], the comprehensive knowledge of GC transcriptional patterns throughout folliculogenesis is limited.

Genomic analyses of germ cells have provided promising insights into the field of developmental biology and reproductive medicine [19]. Among them, the single-cell RNA sequencing (scRNA-seq) has been used to investigate transcriptional alterations of each cell cluster, replacing the conventional bulk sequencing subjected to numerous heterogeneous cells [20, 21]. In the analysis of mouse follicular somatic cell single-cell transcriptomes, there was metabolic reprogramming during GC differentiation [22]. Moreover, sequential and stepwise developmental gene expressions in oocytes, with disturbances of antioxidant signaling specific to early-stage oocytes and granulosa cells, were identified in nonhuman primate ovaries [23]. Notably, spanning over five major follicular stages, the stage-specific expression patterns existed in oocytes and corresponding granulosa cells of human ovaries, which further reflect developmental competency and ovarian reserve [17]. Nevertheless, the transcriptomic data on human ovarian follicles remain incomplete owing to the ethical constraints and limited availability of disease-free human ovarian tissues for research. And deeper understanding of the molecular regulation of human GCs during folliculogenesis will provide invaluable resources for identifying new targets of ovarian disorders.

The dynamic transcriptome is driven by transcription factors (TFs) and noncoding RNAs, all of which comprise a highly resilient regulatory network in the ovaries. As one class of noncoding RNA, long non-coding RNAs (lncRNAs) are transcripts of more than 200 nucleotides, with no significant protein-coding potential [24]. Owing to the regulatory specificity of lncRNA, it promises to serve as biological markers of human disease [24, 25]. It was reported that lncRNA *MALAT1* may be an important regulatory gene affecting granulosa cell proliferation, being related to the manifestations of follicular arrest and adverse pregnancy outcome in women with polycystic ovary syndrome (PCOS) [26]. In women with biochemical premature ovarian insufficiency (bPOI), the expression level of lncRNA *HCP5* was decreased in granulosa cells, which promoted cell apoptosis by impairing DNA damage repair [27]. In addition, numerous studies have pointed out that lncRNAs are extensively involved in other biological processes of follicular development, including granulosa cell expansion, sterol biosynthesis, oocyte nucleoplasm maturation, and chromatin remodeling [28–30]. Therefore, depicting the dynamic lncRNA expression profiles, as well as the mRNA-lncRNA co-expression networks during folliculogenesis, may improve our knowledge of the transcriptional regulation during folliculogenesis.

In the current study, we attempted to shed light on the lncRNA transcriptomic patterns and lncRNA-mRNA co-expression signatures of GCs at different follicular development stages. Moreover, we identified a downregulated *SNHG18* in GCs during ovarian aging, and validated the biological characteristics of lncRNA *SNHG18* in regulating cell proliferation, apoptosis, DNA damage and glycolysis process of granulosa cells via the PKC epsilon (PKCε)/SNHG18/ENO1 pathway. Altogether, our findings brought new insights into the dynamic lncRNA regulation in the folliculogenesis, as well as identified lncRNA *SNHG18* as a novel biomarker of ovarian aging.

Methods

Data preparation

The transcriptome data of 67 GC samples were downloaded from the NCBI Sequence Read Archive (SRA) (GSE107746, https://www.ncbi.nlm.nih.gov/geo/). The GCs were retrieved from human follicles that isolated from fresh ovarian tissues as described previously [17]. SRA Run files were converted to FASTQ format with SRA Tool fastq-dump. Low-quality sequences were trimmed off using FASTX-Toolkit (v.0.0.13; http://hannonlab.cshl.edu/fastx_toolkit/). Then the data quality was assessed using FastQC (http://www.bioinformatics.babraham.ac.uk/projects/fastqc).

Reads alignment and differentially expressed gene (DEG) screening

Clean reads were aligned to the human GRch38 genome using Tophat2 (http://ccb.jhu.edu/software/tophat) with 4 mismatches [31]. Uniquely localized reads were ultimately used to quantify the read counts and reads per kilobase of exon per million reads mapped (RPKM) for each gene. The expression levels of each gene were assessed using RPKM. The software edgeR (http://bioconductor.org) [32], which specifically designed to analyze the differential expression of genes, was applied to the DEGs screening of RNA-seq data. Genes with |log2 fold change (FC)| ≥ 1 and false discovery rate (FDR) ≤ 0.05 between two consecutive stages were identified as DEGs.

In house-script (sogen) was used for data visualization and genomic annotations after the normalization of the reads by TPM (Tags Per Million). The clusters were represented by heatmap package (https://cran.r-project.org/web/packages/pheatmap/index.html) of R.

LncRNA prediction and direction identification

Referring to previous studies [33, 34], a pipeline for lncRNA identification was used to systematically analyze the dynamic expression patterns of lncRNAs. The pipeline was constructed based on the Cufflinks software [35], and the details were as follows: (1) the transcripts were assembled by Cufflinks with the default parameters of follicular development stages, and retained for afterward filtering when FPKM was no less than 0.1; (2) the transcripts were compared with known genes by utilizing Cuffcompare to identify candidate lncRNAs; (3) transcripts with coding potentials were filtered using coding potential calculator (CPC) software; (4) lncRNAs from different developmental stages were merged to the final data set by Cuffmerge; (5) lncRNAs sequence were aligned to databases and named with the best alignment score.

Weighted gene co-expression network (WGCNA) analysis

To fully demonstrate the dynamic expression pattern, WGCNA, with all expressed genes as input data and eigengenes as the representative expression pattern genes in each module, was applied to sort out genes that shared similar expression patterns across folliculogenesis [36]. To further explore the regulatory modes between lncRNAs and their host mRNAs, their relationships were classified into three categories based on the Pearson's correlation coefficients (PCCs) value between mRNA-lncRNA pairs: positive correlated, negative correlated and non-correlated.

Principal component analysis and functional enrichment analysis

Principal component analysis (PCA) analysis was performed by R package factoextra to represent the potential differences of clusters with the first two components. And the DEGs were functionally annotated by Gene Ontology (GO) terms and Kyoto Encyclopedia of Genes and Genomes (KEGG) pathways using the KOBAS 2.0 server [37]. Hypergeometric test and Benjamini-Hochberg FDR controlling procedure were used to define the enrichment of each term. The Reactome pathway database (http://reactome.org) was also utilized for the functional enrichment analysis of selected gene sets.

Animals and single-cell RNA sequencing of mice granulosa cells

Two 13-week-old female and two 52-week-old female C57BL/6J mice were purchased from the SPF Biotechnology Co., Ltd. and bred in the Animal Laboratory Center of Institute of Zoology, Chinese Academy of Sciences in a 12 h light: 12 h darkness cycle with constant temperature and humidity, food and water available ad libitum. All procedures involved were approved by the Animal Research Committee and the Ethics Committee of Beijing Obstetrics and Gynecology Hospital, Capital Medical University.

Unilateral ovaries were dissected out of the female mice for single-cell suspension preparation. Single-cell RNA-seq libraries were constructed using Chromium Next GEM Single Cell 3′ Reagent Kits V3.1 (Dual Index) (10×Genomics). Briefly, Chromium Controller (10×Genomics) was used to generate Gel Beads-in-emulsion (GEMs), post GEM-RT cleanup, cDNA amplification, and cleanup (SPRIselect Reagent Kit). DNAs were ligated to a dual Adaptor (Dual Index Kit TT Set A) following cDNA fragmentation, end preparation, and dA-tailing. The ligated products were amplified, purified, quantified (Qubit 4.0), and stored at -80℃ before sequencing. After that, the ligation products were purified and size fractioned to 300–600 bps. The libraries were prepared according to the manufacturer's instructions and subjected to 150 nt paired-end sequencing using Illumina NovaSeq 6000 system platform. Raw sequencing reads were processed using Cell Ranger. The reference genome for read alignment and quantification was generated following the instructions of 10×Genomics. The other side of the mouse ovary was immersed in 4% paraformaldehyde (PFA) for 6 h, and embedded in paraffin wax after dehydration.

Study participants and human granulosa cells collection

Approved by the Ethics Committee of the Beijing Obstetrics and Gynecology Hospital, Capital Medical University, human granulosa cells isolated from the follicular

fluids were utilized in the following experiments (Code: 2018-KY-066). Sixteen women with bPOI, sixteen women with advanced age, and sixteen normal cycling women who were considered as controls were recruited for this study. The inclusion criteria of bPOI were listed as follows [38]: (1) < 35 years of age; (2) basal serum follicle-stimulating hormone (FSH) ≥ 10 IU/L, serum anti-Müllerian (AMH) < 1.1 ng/mL or ovarian antral follicle counts (AFC) < 5; (3) regular menstruation (23–35 days). The age range of the advanced age group was 35–42 years. Women in the control group were younger than 35 years old and sought infertility treatment for tubal obstruction or male factors. Women with endometriosis, pelvic inflammatory disease, endocrine disorders, recurrent miscarriage, chromosomal abnormality, metabolic syndrome, a history of ovarian surgery or hormone treatment in the past three months were excluded from this study. Informed consents were obtained from all individual participants enrolled in this study.

The follicular fluids were collected at oocyte retrieval from each patient during in vitro fertilization/intracytoplasmic sperm injection and embryo transfer (IVF/ICSI-ET) procedures in the Department of Human Reproductive Medicine, Beijing Obstetrics and Gynecology Hospital, Capital Medical University. The GCs were collected and purified as previously described [39].

Cell culture

SVOG cells (human ovarian granulosa cell line) were utilized for the functional analysis of this study. SVOG cells were maintained in RPMI 1640 medium (GIBCO, Australia) supplemented with 10% FBS (GIBCO) and 1% penicillin-streptomycin (GIBCO), and incubated at 37 °C in a humid atmosphere with 5% CO_2 in the air. To investigate the regulatory roles of PKC epsilon (PKCε) in granulosa cells, PKCε activator DCP-LA or inhibitor Epsilon V1-2 were added to the culture medium of SVOG cells respectively. The cells were treated with DCP-LA 0.1 μM and 1 μM (HY-108599, MCE, USA) and Epsilon-V1-2 1 μM and 10 μM (HY-P0154, MCE) respectively.

Establishment of SVOG cells with stable downexpressing or overexpressing SNHG18

To generate cells stably downexpressing SNHG18, SVOG cells were transfected with small interfering RNAs (siRNAs) or negative control purchased from Ribobio (Guangzhou, China). In brief, SVOG cells were plated in 6-well plates, cultured overnight and transfected using Lipofectamine 3000 Reagent (Invitrogen, California) when the seeded cell to be 50% confluent according to the manufacturer's protocol. The specific sequences were as follows:

$$siRNA - SNHG18\#1, 5$$
$$- CCACTTGGATTTCACCAAA - 3;$$

$$siRNA - SNHG18\#2, 5$$
$$- CCAGAAACTTAGACAGAAA - 3$$

To generate cells stably overexpressing *SNHG18*, *SNHG18* pcDNA 3.1 plasmid or control vector was transfected into SVOG cells using Lipofectamine 3000 when a 70–90% confluence was reached. The expression level of *SNHG18* was detected using quantitative real-time polymerase chain reaction (qRT-PCR).

qRT-PCR

Total RNA was extracted using TRIzol reagent (Invitrogen) and reverse-transcribed into cDNA using TransScript® Green Two-Step qRT-PCR SuperMix (TransGen Biotech, China). The RT-PCR was performed by LightCycler480 real-time PCR system (Roche, Sweden) with PerfectStart® Green qPCR SuperMix (TransGen Biotech). *GAPDH* or *ACTB* was used as an internal control. The relative expression levels were determined using the $2^{-\Delta\Delta Cq}$ method. All of the primer sequences used were listed in Supplementary Table 1.

Western blot analysis

Whole-cell lysates were harvested by radioimmunoprecipitation assay (RIPA) lysis buffer (P0013B, Beyotime, China) supplemented with protease inhibitor cocktail (Roche, Basel, Switzerland) and phosphatase inhibitor (Roche). The cytosolic or nuclear fractions were isolated by Nuclear and Cytoplasmic Protein Extraction Kit (P0028, Beyotime) according to the manufacturer's instructions. As previously described [40], 20 μg was subjected to sodium dodecyl sulfate–polyacrylamide gel electrophoresis (SDS-PAGE). After electrotransferred onto PVDF membranes and blocked with 5% skim milk for 1 h, the membranes were incubated with primary antibodies (Supplementary Table 2) overnight at 4 °C, followed by incubation with horseradish peroxidase (HRP)-conjugated secondary antibodies (Supplementary Table 2) for 1 h at room temperature (RT). The bind intensities were quantified using the enhanced chemiluminescence system (Piece, Rockford, IL). Densitometric quantification was performed using Scion Image software (Scion Corp., USA).

Cell proliferation assay

The cell proliferation assay was conducted using Cell Counting Kit-8 (CCK-8; Lablead, China). *SNHG18* overexpressed or downexpressed SVOG cells were seeded into 96-well culture plates at a density of 2,000 cells/well. Cells transfected with negative control or empty vector were served as control, respectively. After 24, 48 and

72 h incubation, 10 µl CCK-8 solution was added to the culture medium of each well and incubated for an additional 2 h. The absorbance at 450 nm was measured using PerkinElmer/Ensight (USA). The proliferative ability of cells in each group was compared with that of the control group.

EdU assay
According to the manufacturer's instructions, *SNHG18* overexpressed or downexpressed SVOG cells were incubated with 5-ethynyl-20-deoxyuridine (EdU) (Ribobio, China) for 2 h. After being fixed with 4% PFA for 30 min and permeabilized with 0.5% TritonX-100 for 10 min, the cells were incubated with 1×Apollo®567 reaction cocktail for 30 min. The cell nuclei were finally stained with DAPI for 10 min. The images were captured using Zeiss LSM880 (Germany).

Annexin-V apoptosis assay
Cell apoptosis was detected by using an Annexin V- FITC apoptosis Detection Kit (Beyotime) based on the manufacturer's instructions. Briefly, SVOG cells were seeded into six-well plates and cultured overnight, then transfected with *SNHG18* siRNA or overexpressing plasmid. Negative control or empty vector were used as control. The cells were harvested and resuspended with 200 µl binding buffer supplemented with 5 µl Annexin V-FITC and 10 µl PI reagent. After being incubated in the dark for 20 min at RT, the samples were subjected to flow cytometric analysis using BD FACS Aria Fusion (BD Biosciences, USA). Data analysis was performed using FlowJo V8 software (TreeStar, USA).

TUNEL staining
The apoptotic status in *SNHG18* overexpressed or downexpressed SVOG cells were also detected by TdT-mediated dUTP nick end labeling (TUNEL) Apoptosis Assay Kit (Solarbio, China) following the instructions. Briefly, the cells were incubated with TUNEL working solution for 60 min at 37 ℃ and fixed with 4% PFA for 30 min at RT. Then the cell nuclei were stained with DAPI. The images were captured by laser scanning confocal microscope (Zeiss LSM880).

Immunofluorescence
After fixed in 4% PFA for 30 min, *SNHG18* downexpressed SVOG cells were permeabilized in 0.25% Triton X-100 for 10 min and blocked in 2% BSA for 60 min. The cells were incubated with primary antibodies (Supplementary Table 2) at 4 ℃ overnight. Then the cells were incubated with Alexa Fluor secondary antibodies (Supplementary Table 2) for 1 h in the dark at RT. The cell nuclei were stained with DAPI for 10 min.

Paraffin wax-embedded ovaries were then cut into 5-µm-thick slides using a rotary microtome (Leica 2135, Germany). After deparaffinized by a graded alcohol series, the antigen retrieval was performed by boiling the slides in Tris-EDTA buffer for 15 min. Following the blocking with 3% BSA, the slides were incubated with primary antibodies (Supplementary Table 2) at 4 ℃ overnight. The slides were then incubated with Alexa Fluor secondary antibodies (Supplementary Table 2) for 1 h and DAPI for 10 min. The images were captured by Zeiss LSM880.

ATP assay
The ATP levels of *SNHG18* downexpressed SVOG cells were measured using a firefly luciferase-based ATP Assay Kit (Beyotime) according to the manufacturer's instructions. After the cells were lysed and centrifuged at 12,000 × *g* for 5 min, 20 µl supernatant was added to 100 µl ATP detection working dilution in a black 96-well plate. The luminescence of each group was measured using a luminometer (PerkinElmer/Ensight). In order to eliminate the difference caused by the protein content, the protein concentration was detected using the BCA Protein Assay Kit (Beyotime) and microplate reader.

Oxygen consumption rate (OCR) assay
The OCR levels were measured using an Extracellular OCR Plate Assay Kit (DOJINDO, Japan) according to the manufacturer's instructions. In brief, *SNHG18* downexpressed SVOG cells were seeded into 96-well black clear bottom culture plate at a density of 50,000 cells/well and cultured overnight. After removing the culture medium, 100 µl working solution were added into the sample. Then the plate was incubated in microplate reader for 30 min at 37 ℃. After dropping the mineral oil into each well, the fluorescence of sample was recorded at 37 ℃ every 10 min for a total of 200 min, with the default setting as excitation wavelength of 500 nm and emission wavelength of 650 nm.

Extracellular acidification rate (ECAR) assay
The ECAR levels were measured using an Extracellular Acidification Rate (ECAR) Fluorometric Assay Kit (Elabscience, China) according to the manufacturer's instructions. In brief, *SNHG18* downexpressed SVOG cells were seeded into 96-well black clear bottom culture plate at a density of 500,000 cells/well in 100 µl working solution. After incubated in the dark for 30 min at 37 ℃, the samples were detected using a fluorescence microplate reader (PerkinElmer/Ensight). With the default setting as excitation wavelength of 490 nm and emission wavelength of 535 nm, the fluorescence of sample were recorded at 37 ℃ every 5 min for a total of 120 min.

Statistical analysis

Each experiment was performed at least three times independently. Data were represented as mean±standard deviation (SD), and statistically analyzed by R software, GraphPad Prism 10 (GraphPad software, USA), and SPSS 26 (IBM, USA). Comparisons of multiple groups were analyzed by one-way analysis of variance (ANOVA). Student *t*-test and Mann Whitney U test were performed for parametric testing and nonparametric tests respectively between the two groups. Statistically significance was regarded as *P*-value<0.05.

Results

Genome-wide analysis of the dynamic granulosa cell-associated lncRNAs expression during folliculogenesis

To investigate the global expression profiles of granulosa cell-associated lncRNAs, data related to human granulosa cells spanning primordial, primary, secondary, antral and preovulatory stages were retrieved from the Gene Expression Omnibus (GEO) dataset GSE107746 for

analysis. The schematic illustration of the analysis workflow was shown in Fig. 1A. In general, a specific lncRNA expression pattern was shown in each stage of the folliculogenesis (Fig. 1B, Fig. S1A-B), and the total number of differentially expressed (DE) lncRNAs between two consecutive stages appeared to be increased with the progress of follicular development (Fig. 1C). Then to evaluate the variance of lncRNA expression profiles, the obtained RNA-seq normalized RPKM data were subjected to the principal component analysis (PCA). The result showed that samples from the same developmental stages were clustered together based on the lncRNA or mRNA levels (Fig. 1D, Fig. S1C). As listed in Additional file 1, the "granulosa cell-related lncRNA signature" with 18,179 lncRNAs of different stages was described (Fig. S1D-E).

Owing to the diverse expression patterns of lncRNAs displayed during folliculogenesis, the transcriptomic patterns of four lncRNAs being previously reported in GCs and follicles were selected for demonstration (Fig. 1E). Being reported to be the most significantly upregulated
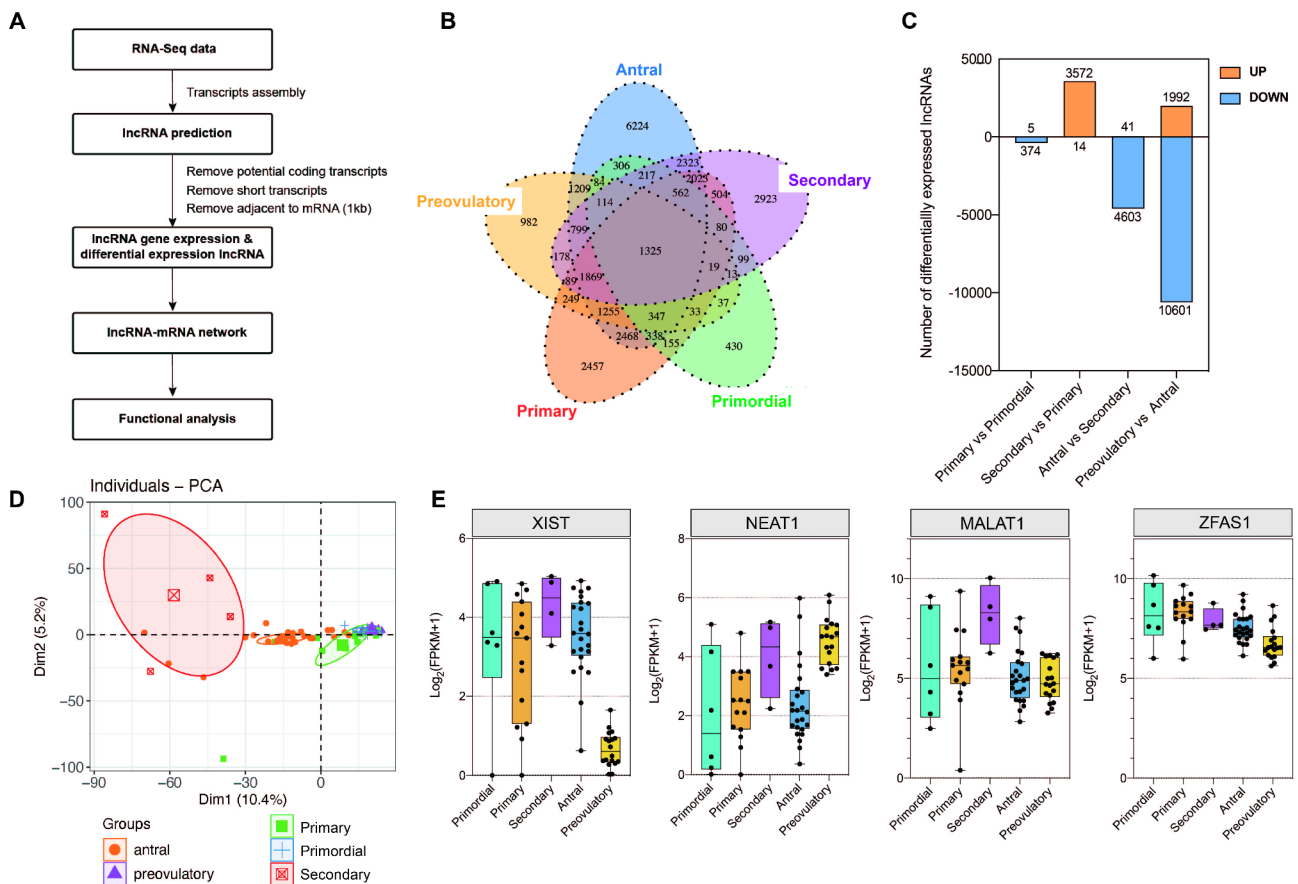

Fig. 1 Dynamic expression of lncRNA signatures in human granulosa cells of different developmental stages. **A**. Experimental design and bioinformatics analysis pipeline of the identification and functional annotation of lncRNAs expressed in human granulosa cells. **B**. Venn diagram of detected lncRNAs at each stage. **C**. Differentially expressed (DE) lncRNAs of consecutive stages: primordial follicle and primary follicle, primary follicle and secondary follicle, secondary follicle and antral follicle, antral follicle and preovulatory follicle. **D**. Principal component analysis (PCA) of 67 samples according to follicular developmental stages based on normalized lncRNAs expression level. **E**. Box plots of the dynamic expression of lncRNA XIST, NEAT1, MALAT1 and ZFAS1 during folliculogenesis

lncRNAs in granulosa cells [29, 41], *XIST* was significantly decreased at the preovulatory stage, while *MALAT1* showed the highest expression level at the secondary stage. *NEAT1*, an architectural lncRNA that constructs paraspeckles and exerts proliferative effects on multiple cancer cells [42, 43], constantly increased until reached the secondary stage. *ZFAS1* decreased as the follicles develop, which was restricted to be expressed in the somatic cells of early antral follicles and reported to inhibit the apoptosis of GCs in PCOS patients [41, 44]. Taken together, distinctive lncRNA expression profile was existed in GCs during folliculogenesis, among which the most variable lncRNA may be employed as stage-specific markers for follicles.

Comprehensive analysis of stage-specific lncRNAs and their co-expressed mRNAs in granulosa cells

To validate the expression patterns of DE lncRNAs, we provided a heatmap of stage-specific lncRNAs in GCs across five follicular developmental stages (Fig. 2A), where lncRNAs separated significantly between different stages. Noticeably, the most abundant DE lncRNAs appeared in the antral follicle stage, indicating an intense transcriptional regulation happened during this period. Since lncRNAs could influence the neighboring coding genes via *cis*-pattern or distant genes via *trans*-pattern [45, 46], mRNA functional modules construction will help to illustrate the biological roles of DE lncRNAs. Therefore, the nearby coding genes around 10 kb up or downstream from the identified lncRNAs were searched to excavate the probable *cis*-regulatory function of DE lncRNAs (Fig. S2A). Thereafter, these co-located genes were subjected to GO enrichment and KEGG pathway analysis, and the top 5 GO terms ($P<0.05$) enriched in molecular function were represented in Fig. 2B, and top 5 KEGG pathways were represented in Fig. S2B. The enriched GO terms reflected the fact that varied lncRNA transcriptome and co-located genes are primarily involved in crucial biological processes at different developmental stages. For instance, genes related to the DNA-dependent regulation of transcription and gene expression processes were enriched in primordial follicles, the positive regulation of epithelial cell proliferation processes enriched in primary/secondary follicles, mitotic cell cycle and chromosome segregation processes in antral follicles, as well as the cellular metabolic process in preovulatory follicles (Fig. 2B). And the enriched KEGG pathways also demonstrated the critical roles of lncRNA and co-located genes in regulating cell cycle and cell metabolism (Fig. S2B).

As for uncovering the unknown functions with biological processes, candidate biomarkers and transcriptional regulatory programs at each stage [47], lncRNA-mRNA co-expression networks were established in our study

(Fig. 2C-G). Through this analysis, we identified a total of 80 correlations with 44 lncRNAs and 38 mRNAs. Moreover, lncRNAs *RP11-5C23.1*, *CTA-276F8.1*, *GNAS-AS1*, *XLOC_214234* and *XLOC_123133* interacted with mRNAs that were closely associated with gametogenesis and steroidogenesis processes. Notably, *SNHG18*, participating in modulating the proliferation and apoptosis of cancer cells [48], was shown to have a robust correlation with *PRKCE* expression (Fig. 2C). And PRKCE was known to be expressed in the cumulus cells and collaborated with anti-apoptotic signaling pathways, which are critical in follicular maturation [49, 50].

Besides, in consideration of the DE lncRNAs abundancy in the antral follicles, we especially focused on the regulatory networks of lncRNA, mRNA, transcription factors (TFs) and cell cycle-related functions at this stage. With four cell cycle-related terms enriched, the network of the 'plateau' profile comprised 123 lncRNAs and 221 mRNAs (Fig. S3). *SKA1* and *TOP2A* showed the top close correlations among the mitotic cell cycle, DNA replication and chromosome segregation pathways. *BLM* was correlated with DNA replication, while *KIF18A* was closely associated with the mitotic cell cycle. Moreover, it was identified that *MIS18BP1* and *E2F3* might serve important roles in mitosis.

Taken together, stage-specific lncRNAs in GCs, in together with their co-expressed mRNAs, are involved in the coordination of granulosa cell functions and follicular development.

WGCNA analysis of expressed lncRNAs and mRNAs in granulosa cells

In screening for the highly correlated lncRNAs associated with folliculogenesis in GCs, WGCNA was utilized for summarizing gene clusters and relating modules to the different developmental stage [36]. The clustering dendrograms detected 5 modules that were significantly correlated with the developmental state of follicles, including MEyellow, MEgrey60 and MEturquoise, MEblack and MEdarkturquoise (Fig. 3A). Specifically, the relationships between the lncRNAs and mRNAs contained in the co-expression modules were displayed in the heatmap across the follicular developmental stages (Fig. 3B). To better understand the roles and functional mechanisms of lncRNAs in these modules, the co-expression networks of mRNA-lncRNA were built with the top 10 of the enriched GO biological processes listed (Fig. 3C-E, Fig. S4A-B). Consistent with the results above, the mitotic cell cycle was the most enriched in the MEyellow and MEgrey60 modules of antral follicles (Fig. 3C-D), while the cellular metabolic process was the most enriched in the MEturquoise module of preovulatory follicles (Fig. 3E). Taken together, the WGCNA results provide additional evidence that GC lncRNA signatures
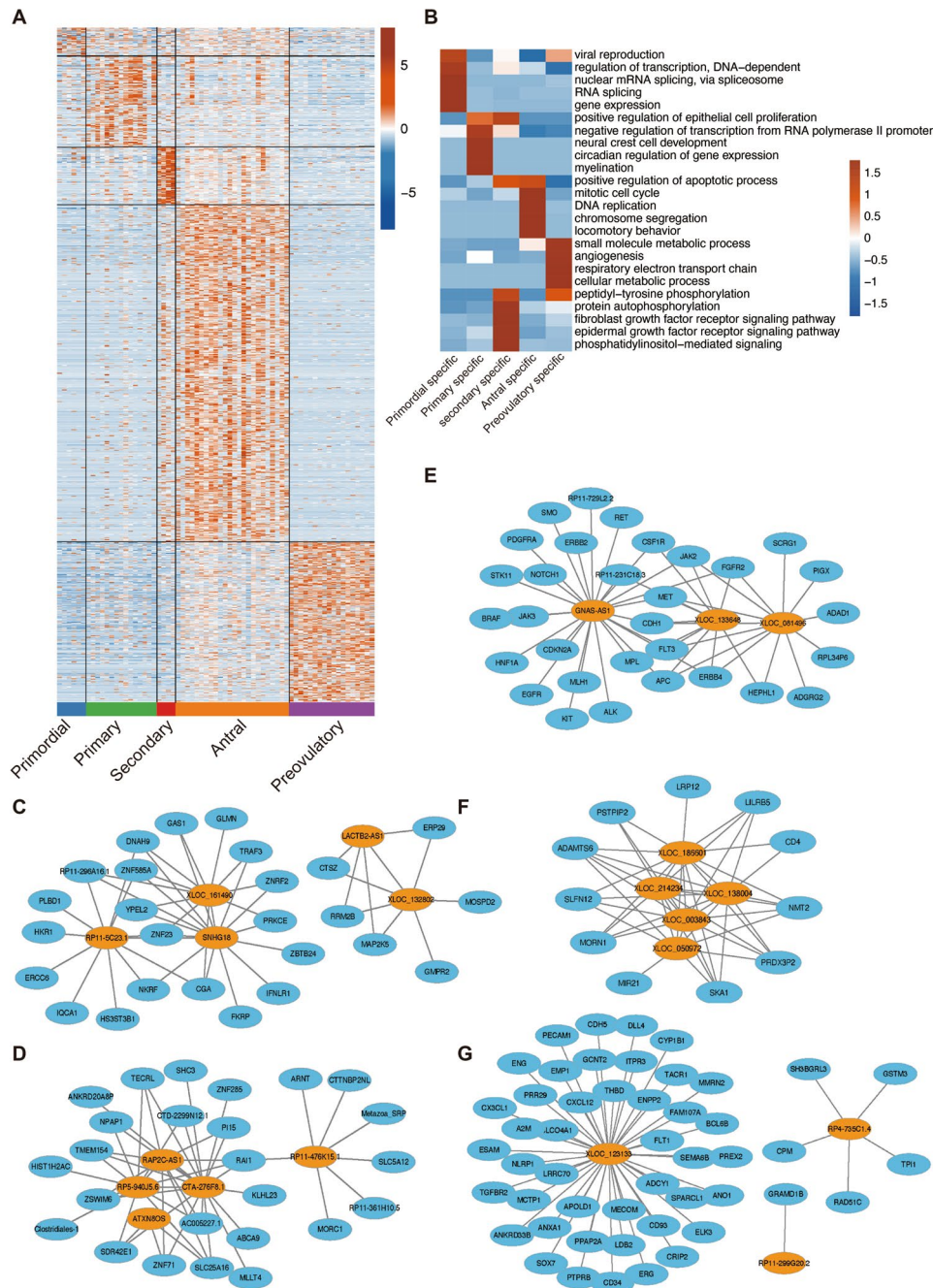
Zhao *et al. Journal of Ovarian Research*   (2024) 17:185

Page 8 of 17

Fig. 2 Co-expression analysis between stage-specific lncRNAs and mRNAs. **A**. Heatmap showing the expression pattern of stage-specific lncRNAs in granulosa cells across five stages of folliculogenesis. The stages of follicular development are presented along with the x-axis. The relative gene expression level from low to high is presented as the color scale from blue to red, respectively. **B**. Top 5 representative GO terms (molecular function) of mRNAs co-expressed with stage-specific lncRNAs at different stages. The row-scaled significance (-$\log_{10}$corrected *P*-value) from low to high is presented as the color scale from blue to red, respectively. C-G. Network diagram identifying the hub lncRNA and co-expressed gene connections among five different developmental stages, primordial follicle (**C**), primary follicle (**D**), secondary follicle (**E**), antral follicle (**F**), preovulatory follicle (**G**)
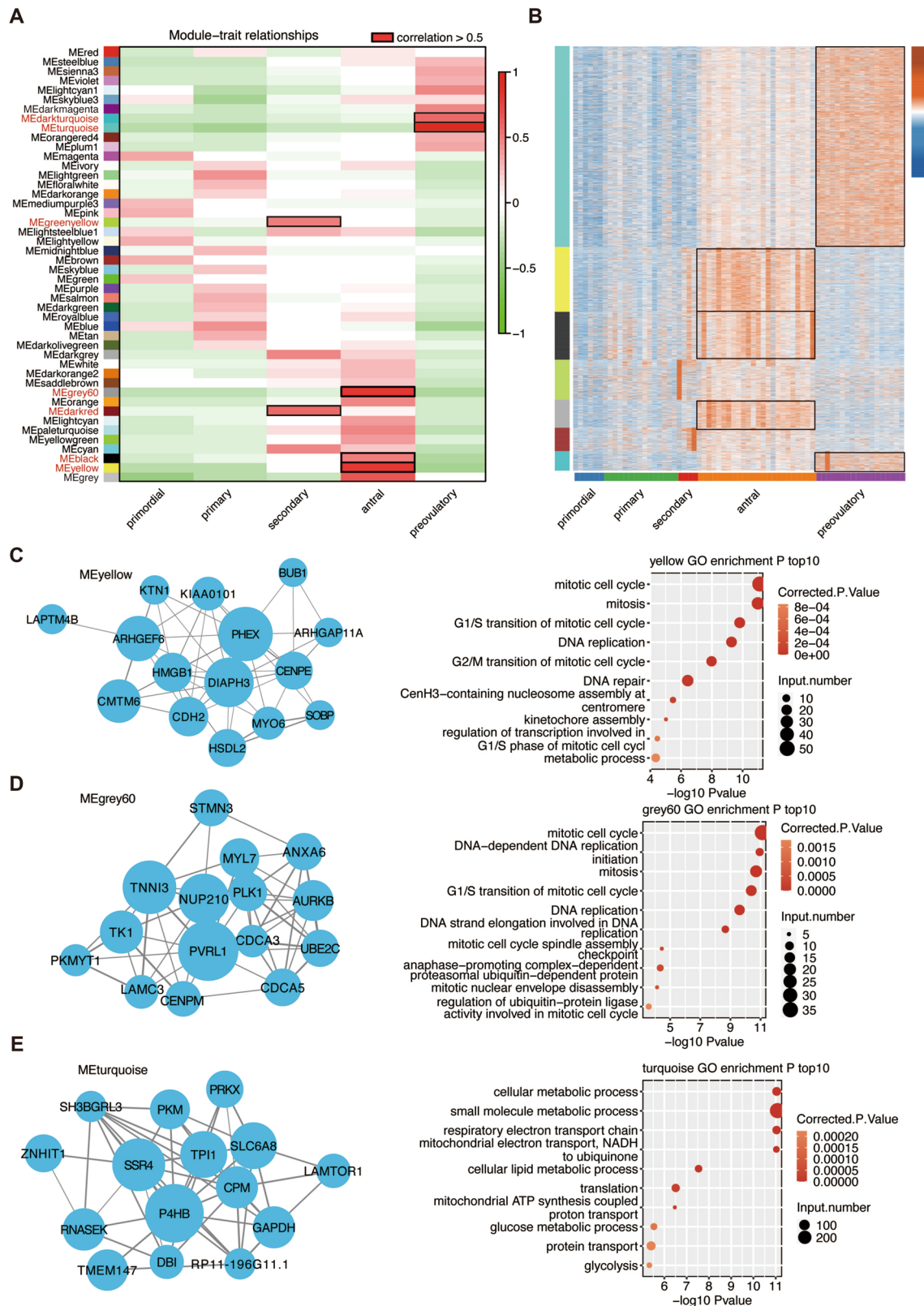
Zhao et al. Journal of Ovarian Research   (2024) 17:185

Page 9 of 17

Fig. 3 WGCNA analysis of expressed lncRNAs and mRNAs during folliculogenesis. **A**. Module-trait associations computed by an LME model with follicular development stages used as covariates. Correlation > 0.5 were framed with black boxes. **B**. Heatmap of lncRNA and mRNA expression levels according to modules framed with black boxes in Fig. 3A. C-E. Module plots displaying the top 15 hub genes, as well as the enriched GO terms in the MEyellow (**C**), MEgrey60 (**D**), MEturquoise (**E**) modules in Fig. 3A

contribute to the mitosis and cellular metabolic process, hence supporting the process of follicular development.

SNHG18 was downregulated in granulosa cells of women with bPOI and advanced age

With the help of single-cell RNA-sequencing results from 13-week and 52-week mouse ovaries (Fig. S5A-B), 36 major clusters of ovarian cells with differentially enriched gene expression patterns were identified in the two groups (Fig. S5C). According to the Supplementary Table 3, we have identified the cell cluster 1, 2, 3, 4, 7, 12, 13, 17, 21, 23, 26, 30, 32, 34 as granulosa cells, and classified them into primordial, antral or preovulatory stages (Fig. S5C). By analyzing the dynamic lncRNA expression profile both in the human granulosa cells and mouse granulosa cells, *SNHG18* and *ZFAS1* existed consistent expression tendencies in follicles across major developmental stages (Fig. 4A-B). Although *SNHG18* is highly expressed in multiple cancer cells and induced radio-resistance in glioma [51, 52], it has been rarely studied in ovarian research. We depicted the expression pattern of *SNHG18* in human GCs at different developmental stages (Fig. 4A). *SNHG18* was highly expressed in GCs at all developmental stages, with an increase during the transition from primordial follicles to primary follicles,

and a subsequent decrease after reaching secondary follicles. Besides, *SNHG18* appeared to be slightly decreased in the antral/preovulatory stage GCs of aging ovaries (Fig. 4B). To further validate whether *SNHG18* plays a crucial role in human ovarian aging, we collected granulosa cells from follicular fluids of bPOI, advanced age, and youthful group, representing the pathological senescence state, physiological senescence states and normal state respectively. The main demographic and clinical characteristics of the studied patients were summarized in Supplementary Table 4. *SNHG18* was significantly decreased in ovarian aging groups after determining by qRT-PCR (Fig. 4C). We further explored the association between the expression of *SNHG18* and AMH, a recognized indicator of ovarian reserve, or female age by Pearson correlation coefficient testing. *SNHG18* was positively correlated with AMH (Fig. 4D), but negatively correlated with female age (Fig. 4E). Taken together, *SNHG18* was downregulated in granulosa cells during ovarian aging, nevertheless, further investigation is needed to determine its precise functions in regulating follicular development and atresia.
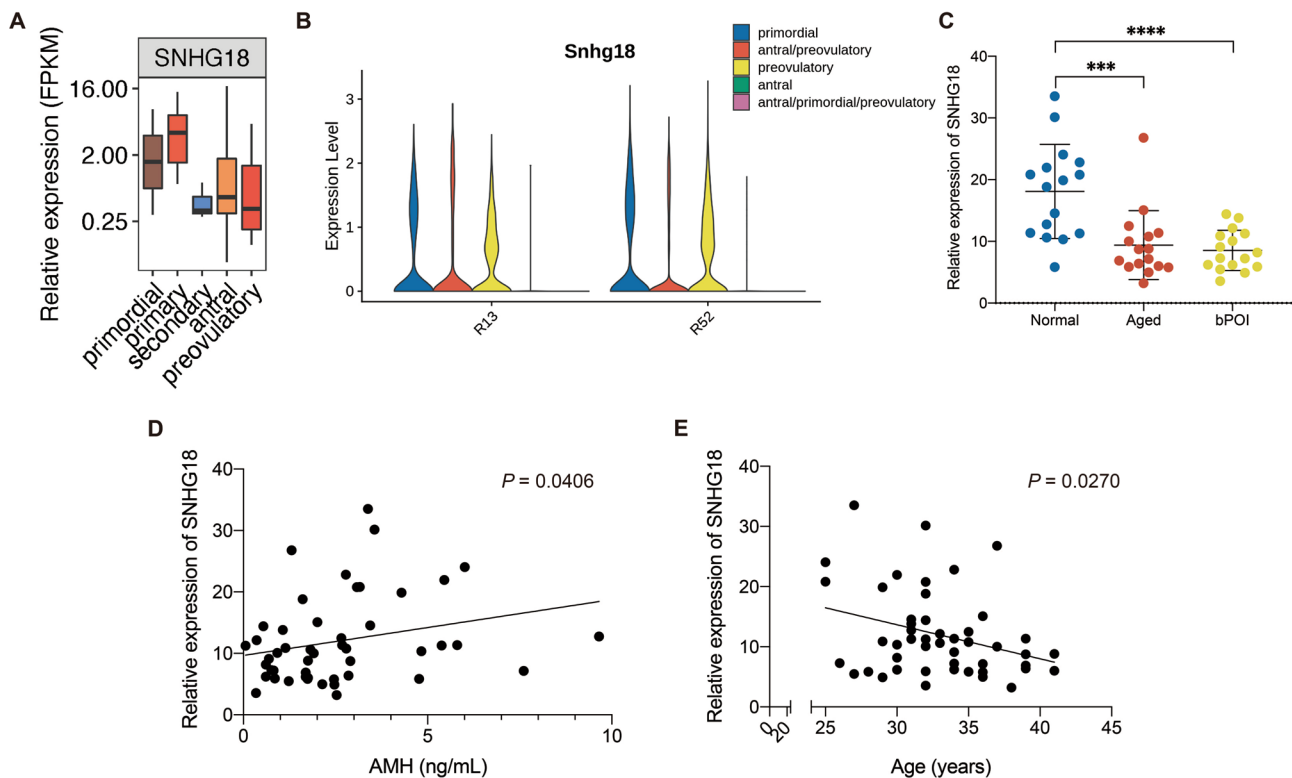

Fig. 4 Expression levels of SNHG18 and their correlation with ovarian aging. **A**. Box plots of the dynamic expression of SNHG18 during folliculogenesis by the previous study. **B**. Violin plot of the relative expression level of lncRNA Snhg18 in single-cell RNA-sequencing data of 13-week and 52-week mouse ovaries. **C**. SNHG18 detection by RT-qPCR in granulosa cells from control, aged and POI women. **D**. The correlation between SNHG18 expression and AMH. E. The correlation between SNHG18 expression and female age. The data were expressed as the mean ± SD. ***, $P < 0.001$; ****, $P < 0.0001$

Downregulated *SNHG18* led to cell apoptosis of human granulosa cells

To clarify the potential roles of *SNHG18* in the follicular development, we further upregulated and downregulated *SNHG18* in SVOG cells with *SNHG18* pcDNA 3.1 plasmids or siRNA transfection (Fig. 5A, Fig. S6A). The apoptosis of cells was detected by TUNEL assay and flow cytometry analysis with Annexin V-FITC/PI staining. In contrast to the negative control group, the proportion of apoptotic cells significantly increased in *SNHG18* siRNA groups (Fig. 5B-C). Moreover, the cell proliferation was detected by EdU and CCK8 assay. We detected decreased number of cells after continuous culturing for 24, 48 and 72 h as determined by CCK8 (Fig. 5D), and a lower ratio of proliferative cells in SNHG18-knockdown groups as determined by EdU (Fig. 5E). After *SNHG18* pcDNA 3.1 plasmids transfection, no significant difference was represented in the apoptosis level of *SNHG18*-overexpressed SVOG cells (Fig. S6B). However, we identified a slight increase in the cell number after culturing for 48 h and 72 h in CCK8 assay (Fig. S6C). Furthermore, there was also an increase of γ-H2A.X in *SNHG18*-downregulated cells (Fig. 5F), indicating the aggravated DNA damage in *SNHG18*-downregulated SVOG cells. Taken together, *SNHG18* down-expression could induce granulosa cell apoptosis, retard cell proliferation, and exacerbate the DNA damage of cells, which may further lead to the follicular atresia in ovarian aging.

Downregulated *SNHG18* by dysregulated PKCε activation could induce glycolysis disruption in granulosa cells

Although some clues about the roles of the PKC signaling pathway in regulating follicles at the intersection of follicle development and atresia [53], PKC isoform ε was seldom mentioned in ovarian studies [49]. Taking into account the co-expression of *PRKCE* and *SNHG18*, we further detected the *PRKCE* expression in human GC samples. As expected, *PRKCE* mRNA was significantly reduced in the aged group, though no significant difference was identified in bPOI patients (Fig. 6A). To investigate whether PKCε activation is involved in *SNHG18* expression, PKCε activator DCP-LA or inhibitor Epsilon V1-2 were added to the culture medium of SVOG cells seperately. After supplemented with DCP-LA 0.1 μM or 1 μM, an increased *SNHG18* expression was identified in SVOG cells (Fig. 6B, D). When PKCε activation was selectively inhibited by Epsilon V1-2, the expression of *SNHG18* was reduced conversely in the 1 μM or 10 μM Epsilon V1-2 groups (Fig. 6C-D). However, *SNHG18* overexpression failed to altered the expression of *PRKCE* (Fig. S6D).

Considering that *SNHG18* participates in cancer progression by modulating the efficiency of glycolysis process [54] and the great metabolic needs during folliculogenesis, the ATP production was next determined in our study. We monitored a decrease in ATP production in *SNHG18*-knockdown SVOG cells (Fig. 7A). Moreover, the ECAR and OCR levels were also reduced in *SNHG18*-knockdown SVOG cells (Fig. 7B-C). Thereafter, we examined the expression levels of genes encoding key glycolytic enzymes in *SNHG18*-knockdown SVOG cells, which turned out that α-Enolase 1 (ENO1) might be specifically downregulated by the *SNHG18* down-expression (Fig. 7D-E, Fig. S7A).

By investigating the granulosa cell samples from patients, we discovered that *ENO1* expression was also significantly decreased in ovarian aging groups (Fig. 7F), and positively correlated with the expression of *SNHG18* (Fig. 7G). Moreover, ENO1 decreased in the granulosa cells among antral follicles from 52-week mice ovary when compared with 13-week mice (Fig. 7H). Previous studies have revealed a strong relationship between the cellular location of lncRNAs and their regulatory functions [55]. Similarly, the multiple functions and positions of ENO1 in cells are also inseparable [56]. Therefore, we explored the alterations of ENO1 subcellular localization induced by down-regulated *SNHG18*. Decreased levels of ENO1 protein were observed both in the nucleus and cytoplasm of *SNHG18*-knockdown SVOG cells (Fig. 7I-J). Furthermore, PKCε activation increased the total ENO1 level in granulosa cells, while decreased ENO1 level was observed after PKCε inactivation (Fig. S7B-C). Taken together, downregulated expression of *SNHG18* may reduce the expression of ENO1 in the granulosa cells, thereby affecting the proliferation and apoptosis of granulosa cells.

Discussion

Deeper understanding of dynamic transcriptomics during follicular development will provide invaluable resources for identifying new biomarkers and targets of ovarian disorders. Despite many studies displayed the essential roles of genetic and epigenetic factors in regulating folliculogenesis [10, 17], a genome-scale lncRNAs analysis of human granulosa cells are challenging. In this study, the specific GC-associated lncRNAs profiles across different developmental stages were depicted, demonstrating their abilities in coordinating the granulosa cell functions and follicular development. Next, *SNHG18* participated in the pathogenesis of ovarian aging, while PKCε expression and activation retained a strong relationship with *SNHG18*. Moreover, downregulated PKCε/SNHG18 pathway furtherly interrupted the glycolysis of granulosa cells by reducing the ENO1 protein.

Ovarian aging is mainly characterized by a gradual loss of the quantity and quality of oocytes, encompassing physiological aging that brought on by age, and pathological aging that brought on by multiple factors
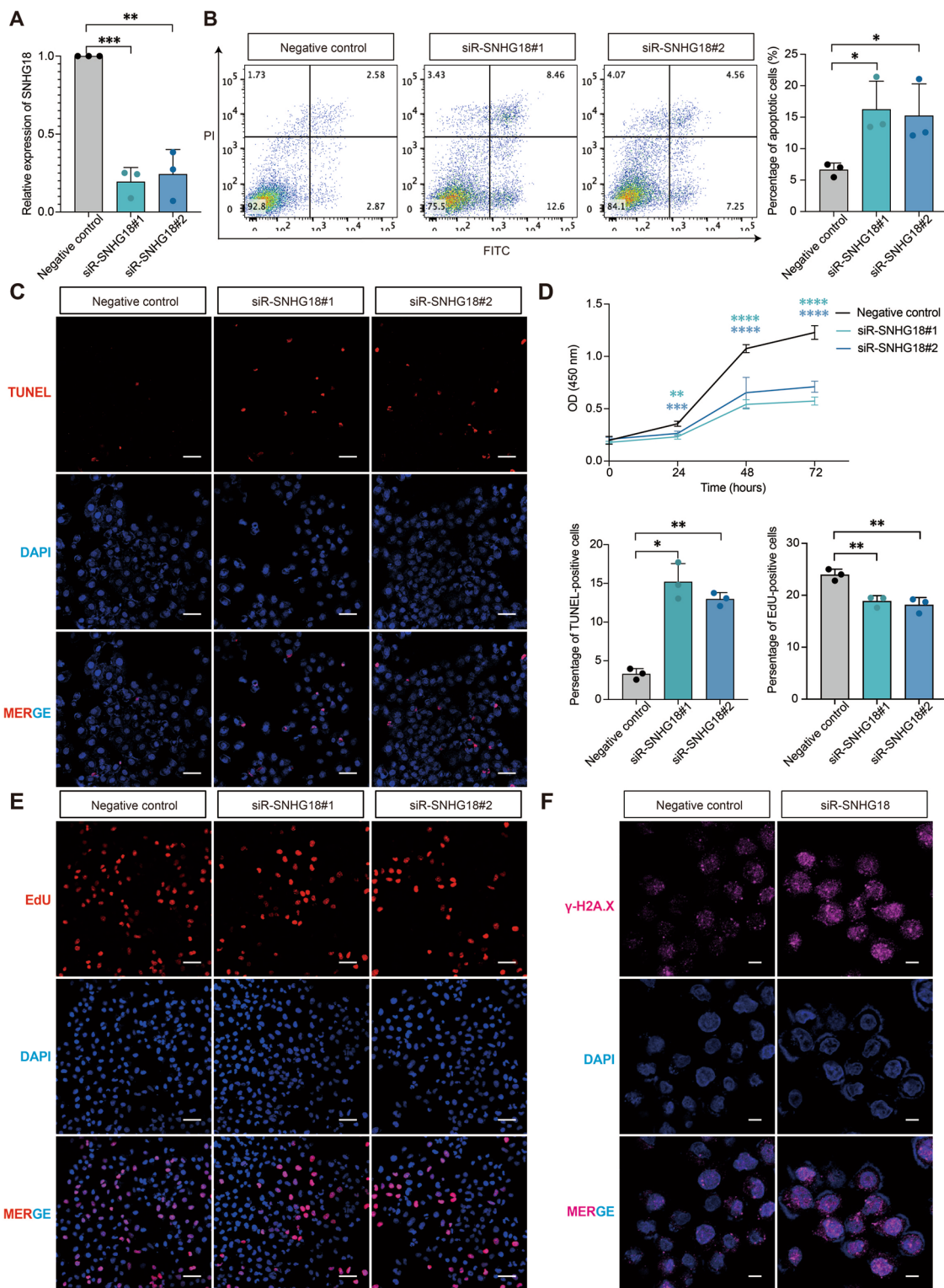
Fig. 5 Downregulated SNHG18 inhibited cell viability and induced apoptosis of granulosa cells. **A**. Decreased expression of SNHG18 in SNHG18-knock-down SVOG cells detected by RT-qPCR. **B**. Annexin V-FITC/PI staining and flow-cytometry analysis of the proportion of apoptotic cells. **C**. TUNEL staining of the apoptotic cells. TUNEL-positive cells, red; cell nuclei, blue. Scale bars, 50 μm. (**D**) CCK8 assay of the SNHG18-knockdown SVOG cells. (**E**) EdU staining of the proliferative cells in SNHG18-knockdown SVOG cells. EdU-positive cells, red; cell nuclei, blue. Scale bars, 50 μm. (**F**) γ-H2A.X immunofluorescence of the SNHG18-knockdown SVOG cells. γ-H2A.X, pink; cell nuclei, blue. Scale bars, 10 μm. All of the experiments were performed in triplicate at least and the data were expressed as the mean ± SD. *, $P < 0.05$; **, $P < 0.01$; ***, $P < 0.001$; ****, $P < 0.0001$
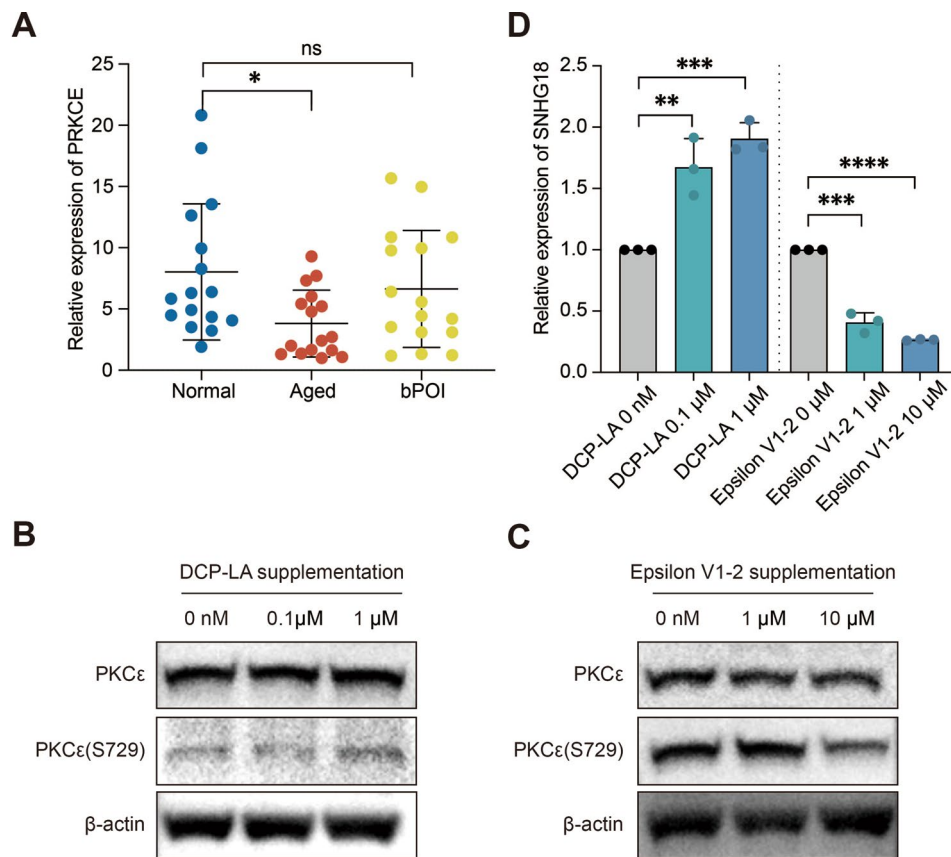
Fig. 6 Regulation of PKCε activation on downstream molecules. **A**. PRKCE expression detection by RT-qPCR in granulosa cells from control, aged and POI women. **B**. Western blotting detection of the PKCε, PKCε(S729) level after supplementation with DCP-LA. (**C**) Western blotting detection of the PKCε, PKCε(S729) level after supplementation with Epsilon V1-2. (**D**) The relative expression level of SNHG18 after supplementation with DCP-LA or Epsilon V1-2. All of the experiments were performed in triplicate at least and the data were expressed as the mean ± SD. **, $P < 0.01$; ***, $P < 0.001$; ****, $P < 0.0001$

[57, 58]. Ovarian aging arises from the accelerated rate of follicle consumption, while granulosa cell apoptosis and follicular atresia are intricately related to ovarian reserve depletion [13, 14]. Although the specific mechanism concerning the biological processes in ovarian aging is unclear, dysregulated follicular activation, recruitment, and development are reported be related [1]. Since lncRNAs are widely known for exerting their effects in normal folliculogenesis and ovarian disorders by serving as transcription factors, histone modification complexes, miRNAs, and protein stabilizers [59], lncRNA characterization is pivotal to both physiological and premature ovarian aging [60, 61]. Our current work revealed that the expression of *SNHG18* was downregulated in the granulosa cells of women with POI or advanced maternal age, and showed a positive correlation with ovarian reserve. This suggested that *SNHG18* may serve as a diagnostic biomarker of ovarian aging. As indicated by previous studies, *SNHG18* had the ability to support the radio-resistance, migration and invasion of glioma [51, 54]. Knockdown of *SNHG18* expression using siRNAs significantly suppressed the proliferation and promote

the apoptosis of SVOG cells, indicating that *SNHG18* may exacerbate the follicular atresia in ovaries.

The importance of PKC signaling in the regulation of follicular development, especially the major functions in mediating cell differentiation, cytokine activation and negative regulation of apoptotic process in GCs, have been confirmed in a few studies [53, 62]. We detected that SNHG18 retained a strong relationship with *PRKCE* expression, and PKCε activation acted as a critical part in terms of maintaining GC proliferation by regulating *SNHG18*. As small nucleolar RNA host genes (SNHGs) played pivotal roles in cancer cell growth and progression [63–65], which was closely related to the glycolysis process. Moreover, *SNHG18* has been confirmed to mainly locate in the nucleus and interact with the nuclear protein ENO1 [54]. Acting as a glycolytic enzyme, ENO1 also exhibits other activities that strongly depend on its cellular and extracellular localization [56]. ENO1 participated in the glycolysis in cytoplasm, while taking part in the transcription regulation of cancer cell proliferation in the nucleus. Currently, we found that the disruption of the PKCε/SNHG18 pathway in ovarian aging led to the
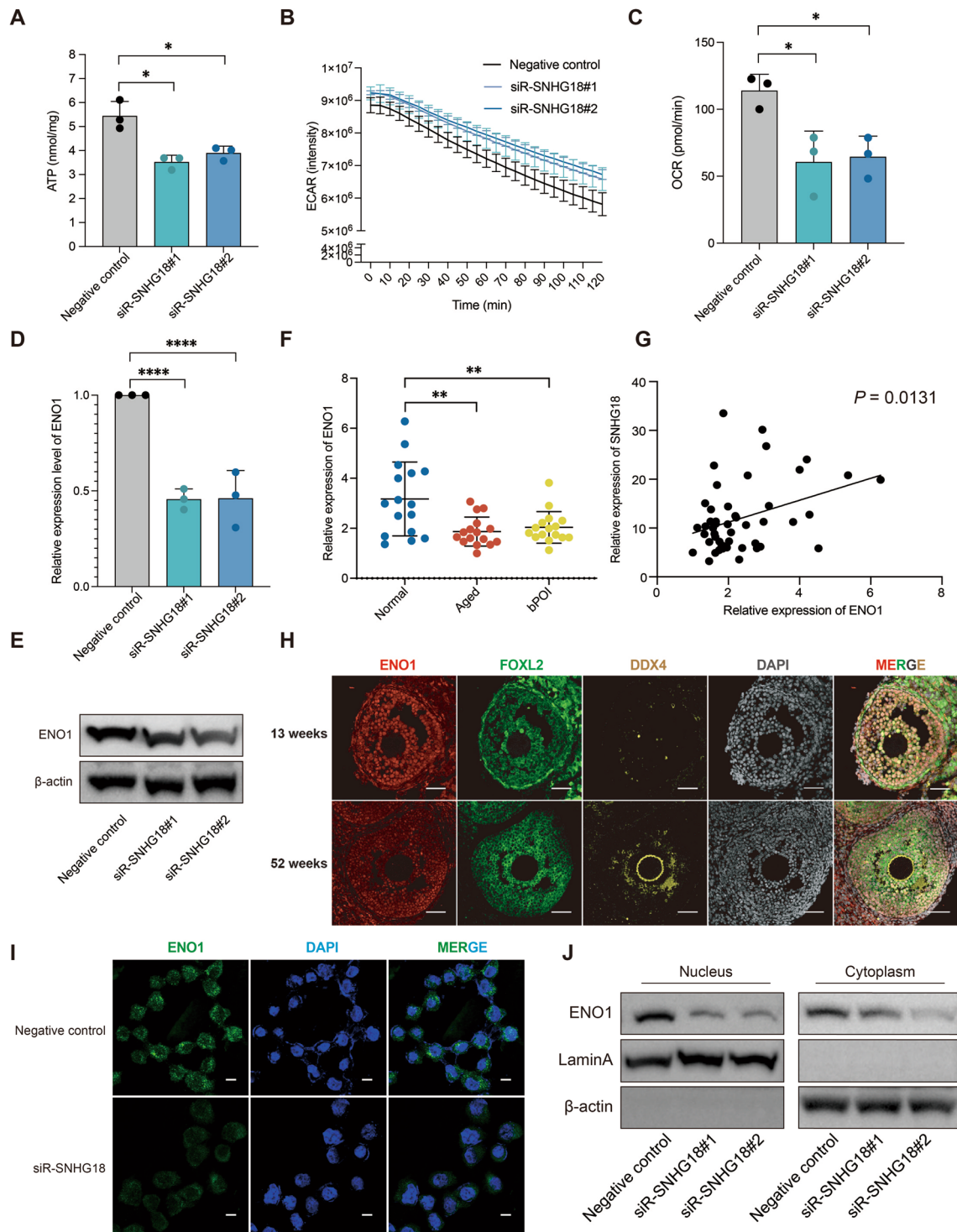
Fig. 7 Downregulated SNHG18 by inhibited PKCε activation interfered with glycolysis via regulating ENO1 subcellular expression. **A**. ATP detection of SNHG18-knockdown SVOG cells. **B**. ECAR level detection of SNHG18-knockdown SVOG cells. **C**. OCR level of SNHG18-knockdown SVOG cells. **D**. The expression of ENO1 mRNA in SNHG18-knockdown SVOG cells. **E**. Western blotting detection of the total ENO1 level of SNHG18-knockdown SVOG cells. **F**. ENO1 detection by RT-qPCR in human primary granulosa cells from control, aged and POI women. **G**. The correlation between SNHG18 expression and ENO1 mRNA expression. **H**. ENO1 immunofluorescence in 13-week and 52-week mouse ovaries. ENO1, red; FOXL2, green; DDX4, yellow; DAPI, grey. **I**. ENO1 immunofluorescence of SNHG18-KD SVOG cells. ENO1, green; DAPI, blue. Scale bars, 10 μm. **J**. Western blotting detection of the nucleus and cytoplasm ENO1 level of SNHG18-knockdown SVOG cells. All of the experiments were performed in triplicate at least and the data were expressed as the mean ± SD. **, $P < 0.01$; ****, $P < 0.0001$

Zhao *et al. Journal of Ovarian Research*　　(2024) 17:185

Page 15 of 17

granulosa cells apoptosis by reducing the ENO1 expression in both the nucleus and cytoplasm, thereby interrupting with glycolysis and cell proliferation.

Since the primary granulosa cells obtained from in vitro fertilization procedures are generally collected 36 h after human chorionic gonadotropin (hCG) administration, which makes it difficult for these luteinized granulosa cells to survive for extended cell generations. In order to identify the regulatory roles of *SNHG18* in ovarian aging, adequate numbers of homogenous granulosa cell populations are needed. Currently, the SVOG cell line was used in our study for it preserves the majority of the pattern of human granulosa cells. However, further studies to replicate these findings with the primary human granulosa cells are needed.

Conclusions

In conclusion, our study demonstrated that the specific transcriptome of GC-associated lncRNAs across different developmental stages exhibits crucial biological functions. And downregulated PKCε/SNHG18 pathway may promote granulosa cell apoptosis via interruption of glycolysis by ENO1, participating in the pathogenesis of ovarian aging. Hence, we proved that *SNHG18* may serve as a novel biomarker of ovarian aging and provided new perspectives in illustrating the regulatory mechanisms of follicular atresia.

Abbreviations

lncRNA	Long non-coding ribonucleic acid
GC	Granulosa cell
scRNA-seq	Single-cell RNA sequencing
TF	Transcription factor
PCOS	Polycystic ovary syndrome
bPOI	Biochemical premature ovarian insufficiency
PKCε	PKC epsilon
SRA	Sequence Read Archive
DEG	Differentially expressed gene
RPKM	Per kilobase of exon per million reads mapped
FC	Fold change
FDR	False discovery rate
TPM	Tags Per Million
WGCNA	Weighted gene co-expression network
PCC	Pearson's correlation coefficient
PCA	Principal component analysis
GO	Gene Ontology
KEGG	Kyoto Encyclopedia of Genes and Genomes
GEMs	Gel Beads-in-emulsion
PFA	Paraformaldehyde
FSH	Follicle-stimulating hormone
AMH	Anti-Müllerian
AFC	Antral follicle count
IVF/ICSI-ET	In vitro fertilization/intracytoplasmic sperm injection and embryo transfer
SVOG	Human ovarian granulosa cell line
siRNA	Small interfering RNA
qRT-PCR	Quantitative real-time polymerase chain reaction
RIPA	Radioimmunoprecipitation assay
SDS-PAGE	Sodium dodecyl sulfate–polyacrylamide gel electrophoresis
RT	Room temperature
CCK-8	CELL Counting Kit-8
CCK-8	5-Ethynyl-20-deoxyuridine
TUNEL	TdT-mediated dUTP nick end labeling
SD	Standard deviation
ANOVA	One-way analysis of variance
GEO	GENE Expression Omnibus
DE	Differentially expressed
SNHG	Small nucleolar RNA host gene

Supplementary Information

The online version contains supplementary material available at https://doi.org/10.1186/s13048-024-01510-4.

Supplementary Material 1

Supplementary Material 2

Supplementary Material 3

Data availability
No datasets were generated or analysed during the current study.

Declarations

Ethics approval and consent to participate
All experiments were approved by the Ethics Committee of the Beijing Obstetrics and Gynecology Hospital, Capital Medical University for the collection of human granulosa cells (Code: 2018-KY-066). Informed consent was obtained from all individual participants included in the study.

Consent for publication
Not applicable.

Competing interests
The authors declare no competing interests.

References
1. Laisk T, Tšuiko O, Jatsenko T, Hõrak P, Otala M, Lahdenperä M, et al. Demographic and evolutionary trends in ovarian function and aging. Hum Reprod Update. 2019;25(1):34–50.
2. Richani D, Dunning KR, Thompson JG, Gilchrist RB. Metabolic co-dependence of the oocyte and cumulus cells: essential role in determining oocyte developmental competence. Hum Reprod Update. 2021;27(1):27–47.
3. Dumesic DA, Meldrum DR, Katz-Jaffe MG, Krisher RL, Schoolcraft WB. Oocyte environment: follicular fluid and cumulus cells are critical for oocyte health. Fertil Steril. 2015;103(2):303–16.

4.   Sutton-McDowall ML, Gilchrist RB, Thompson JG. The pivotal role of glucose metabolism in determining oocyte developmental competence. Reproduction. 2010;139(4):685–95.

5.   Gilchrist RB, Lane M, Thompson JG. Oocyte-secreted factors: regulators of cumulus cell function and oocyte quality. Hum Reprod Update. 2008;14(2):159–77.

6.   Buratini J, Dellaqua TT, Dal Canto M, La Marca A, Carone D, Mignini Renzini M, et al. The putative roles of FSH and AMH in the regulation of oocyte developmental competence: from fertility prognosis to mechanisms underlying age-related subfertility. Hum Reprod Update. 2022;28(2):232–54.

7.   Macaulay AD, Gilbert I, Scantland S, Fournier E, Ashkar F, Bastien A, et al. Cumulus cell transcripts transit to the bovine oocyte in Preparation for Maturation. Biol Reprod. 2016;94(1):16.

8.   Santonocito M, Vento M, Guglielmino MR, Battaglia R, Wahlgren J, Ragusa M, et al. Molecular characterization of exosomes and their microRNA cargo in human follicular fluid: bioinformatic analysis reveals that exosomal microRNAs control pathways involved in follicular maturation. Fertil Steril. 2014;102(6):1751–61.

9.   Hussein MR. Apoptosis in the ovary: molecular mechanisms. Hum Reprod Update. 2005;11(2):162–77.

10. Zhang J, Xu Y, Liu H, Pan Z. MicroRNAs in ovarian follicular atresia and granulosa cell apoptosis. Reprod Biol Endocrinol. 2019;17(1):9.

11. Johnson MT, Freeman EA, Gardner DK, Hunt PA. Oxidative metabolism of pyruvate is required for meiotic maturation of murine oocytes in vivo. Biol Reprod. 2007;77(1):2–8.

12. Li R, Albertini DF. The road to maturation: somatic cell interaction and self-organization of the mammalian oocyte. Nat Rev Mol Cell Biol. 2013;14(3):141–52.

13. Alberico HC, Woods DC. Role of Granulosa cells in the Aging Ovarian Landscape: a focus on mitochondrial and metabolic function. Front Physiol. 2021;12:800739.

14. Tatone C, Amicarelli F. The aging ovary–the poor granulosa cells. Fertil Steril. 2013;99(1):12–7.

15. Yeung CK, Wang G, Yao Y, Liang J, Tenny Chung CY, Chuai M, et al. BRE modulates granulosa cell death to affect ovarian follicle development and atresia in the mouse. Cell Death Dis. 2017;8(3):e2697.

16. Jiao X, Ke H, Qin Y, Chen ZJ. Molecular Genetics of premature ovarian insufficiency. Trends Endocrinol Metab. 2018;29(11):795–807.

17. Zhang Y, Yan Z, Qin Q, Nisenblat V, Chang HM, Yu Y, et al. Transcriptome landscape of human folliculogenesis reveals oocyte and granulosa cell interactions. Mol Cell. 2018;72(6):1021–34.

18. Yang J, Li Y, Li S, Zhang Y, Feng R, Huang R, et al. Metabolic signatures in human follicular fluid identify lysophosphatidylcholine as a predictor of follicular development. Commun Biol. 2022;5(1):763.

19. La H, Yoo H, Lee EJ, Thang NX, Choi HJ, Oh J, et al. Insights from the applications of single-cell transcriptomic analysis in germ cell development and reproductive medicine. Int J Mol Sci. 2021;22(2):823.

20. Sohni A, Tan K, Song HW, Burow D, de Rooij DG, Laurent L, et al. The neonatal and adult human testis defined at the single-cell level. Cell Rep. 2019;26(6):1501–17.

21. Wang M, Liu X, Chang G, Chen Y, An G, Yan L, et al. Single-cell RNA sequencing analysis reveals sequential cell fate transition during human spermatogenesis. Cell Stem Cell. 2018;23(4):599–614.

22. Li S, Chen LN, Zhu HJ, Feng X, Xie FY, Luo SM, et al. Single-cell RNA sequencing analysis of mouse follicular somatic cells†. Biol Reprod. 2021;105(5):1234–45.

23. Wang S, Zheng Y, Li J, Yu Y, Zhang W, Song M, et al. Single-cell transcriptomic atlas primate ovarian aging. Cell. 2020;180(3):585–600.

24. Kopp F, Mendell JT. Functional classification and experimental dissection of long noncoding RNAs. Cell. 2018;172(3):393–407.

25. Guttman M, Rinn JL. Modular regulatory principles of large non-coding RNAs. Nature. 2012;482(7385):339–46.

26. Tu M, Wu Y, Wang F, Huang Y, Qian Y, Li J, et al. Effect of lncRNA MALAT1 on the Granulosa cell proliferation and pregnancy outcome in patients with PCOS. Front Endocrinol (Lausanne). 2022;13:825431.

27. Wang X, Zhang X, Dang Y, Li D, Lu G, Chan WY, et al. Long noncoding RNA HCP5 participates in premature ovarian insufficiency by transcriptionally regulating MSH5 and DNA damage repair via YB1. Nucleic Acids Res. 2020;48(8):4480–91.

28. Ouandaogo ZG, Frydman N, Hesters L, Assou S, Haouzi D, Dechaud H, et al. Differences in transcriptomic profiles of human cumulus cells isolated from oocytes at GV, MI and MII stages after in vivo and in vitro oocyte maturation. Hum Reprod. 2012;27(8):2438–47.

29. Bouckenheimer J, Fauque P, Lecellier CH, Bruno C, Commes T, Lemaître JM, et al. Differential long non-coding RNA expression profiles in human oocytes and cumulus cells. Sci Rep. 2018;8(1):2202.

30. Yerushalmi GM, Salmon-Divon M, Yung Y, Maman E, Kedem A, Ophir L, et al. Characterization of the human cumulus cell transcriptome during final follicular maturation and ovulation. Mol Hum Reprod. 2014;20(8):719–35.

31. Kim D, Pertea G, Trapnell C, Pimentel H, Kelley R, Salzberg SL. TopHat2: accurate alignment of transcriptomes in the presence of insertions, deletions and gene fusions. Genome Biol. 2013;14(4):R36.

32. Robinson MD, McCarthy DJ, Smyth GK. edgeR: a Bioconductor package for differential expression analysis of digital gene expression data. Bioinformatics. 2010;26(1):139–40.

33. Liu S, Wang Z, Chen D, Zhang B, Tian RR, Wu J, et al. Annotation and cluster analysis of spatiotemporal- and sex-related lncRNA expression in rhesus macaque brain. Genome Res. 2017;27(9):1608–20.

34. Cabili MN, Trapnell C, Goff L, Koziol M, Tazon-Vega B, Regev A, et al. Integrative annotation of human large intergenic noncoding RNAs reveals global properties and specific subclasses. Genes Dev. 2011;25(18):1915–27.

35. Trapnell C, Roberts A, Goff L, Pertea G, Kim D, Kelley DR, et al. Differential gene and transcript expression analysis of RNA-seq experiments with TopHat and Cufflinks. Nat Protoc. 2012;7(3):562–78.

36. Langfelder P, Horvath S. WGCNA: an R package for weighted correlation network analysis. BMC Bioinformatics. 2008;9:559.

37. Xie C, Mao X, Huang J, Ding Y, Wu J, Dong S, et al. KOBAS 2.0: a web server for annotation and identification of enriched pathways and diseases. Nucleic Acids Res. 2011;39:W316–22.

38. Welt CK. Primary ovarian insufficiency: a more accurate term for premature ovarian failure. Clin Endocrinol (Oxf). 2008;68(4):499–509.

39. Zhao F, Wu L, Wang Q, Zhao X, Chen T, Yin C, et al. Insulin-like growth factor 2 mRNA-binding protein 2-regulated alternative splicing of nuclear factor 1 C-type causes excessive granulosa cell proliferation in polycystic ovary syndrome. Cell Prolif. 2022;55(4):e13216.

40. Yang X, Zhou Y, Peng S, Wu L, Lin HY, Wang S, et al. Differentially expressed plasma microRNAs in premature ovarian failure patients and the potential regulatory function of mir-23a in granulosa cell apoptosis. Reproduction. 2012;144(2):235–44.

41. Ernst EH, Nielsen J, Ipsen MB, Villesen P, Lykke-Hartmann K. Transcriptome analysis of long non-coding RNAs and genes encoding paraspeckle proteins during human ovarian follicle development. Front Cell Dev Biol. 2018;6:78.

42. Yamazaki T, Souquere S, Chujo T, Kobelke S, Chong YS, Fox AH, et al. Functional domains of NEAT1 architectural lncRNA induce paraspeckle assembly through phase separation. Mol Cell. 2018;70(6):1038–53.

43. Wang S, Zuo H, Jin J, Lv W, Xu Z, Fan Y, et al. Long noncoding RNA Neat1 modulates myogenesis by recruiting Ezh2. Cell Death Dis. 2019;10(7):505.

44. Zhu HL, Chen YQ, Zhang ZF. Downregulation of lncRNA ZFAS1 and upregulation of microRNA-129 repress endocrine disturbance, increase proliferation and inhibit apoptosis of ovarian granulosa cells in polycystic ovarian syndrome by downregulating HMGB1. Genomics. 2020;112(5):3597–608.

45. Rinn JL, Chang HY. Genome regulation by long noncoding RNAs. Annu Rev Biochem. 2012;81:145–66.

46. Gil N, Ulitsky I. Regulation of gene expression by cis-acting long non-coding RNAs. Nat Rev Genet. 2020;21(2):102–17.

47. van Dam S, Võsa U, van der Graaf A, Franke L, de Magalhães JP. Gene co-expression analysis for functional classification and gene-disease predictions. Brief Bioinform. 2018;19(4):575–92.

48. Ma Q, Yang T. E2F transcription factor 1/small nucleolar RNA host gene 18/microRNA-338-5p/forkhead box D1: an important regulatory axis in glioma progression. Bioengineered. 2022;13(1):418–30.

49. Tepekoy F, Ustunel I, Akkoyunlu G. Protein kinase C isoforms α, δ and ε are differentially expressed in mouse ovaries at different stages of postnatal development. J Ovarian Res. 2014;7:117.

50. Maraldi T, Riccio M, Sena P, Marzona L, Nicoli A, La Marca A, et al. MATER protein as substrate of PKCepsilon in human cumulus cells. Mol Hum Reprod. 2009;15(8):499–506.

51. Zheng R, Yao Q, Ren C, Liu Y, Yang H, Xie G, et al. Upregulation of long noncoding RNA small nucleolar RNA host gene 18 promotes Radioresistance of Glioma by repressing semaphorin 5A. Int J Radiat Oncol Biol Phys. 2016;96(4):877–87.

Zhao et al. Journal of Ovarian Research   (2024) 17:185

Page 17 of 17

52. Fan H, Yuan J, Li Y, Jia Y, Li J, Wang X, et al. MKL1-induced lncRNA SNHG18 drives the growth and metastasis of non-small cell lung cancer via the miR-211-5p/BRD4 axis. Cell Death Dis. 2021;12(1):128.

53. Tremblay PG, Sirard MA. Gene analysis of major signaling pathways regulated by gonadotropins in human ovarian granulosa tumor cells (KGN)†. Biol Reprod. 2020;103(3):583–98.

54. Zheng R, Yao Q, Li X, Xu B. Long noncoding ribonucleic acid SNHG18 promotes glioma cell motility via disruption of α-Enolase nucleocytoplasmic transport. Front Genet. 2019;10:1140.

55. Zhu Y, Jin L, Shi R, Li J, Wang Y, Zhang L, et al. The long noncoding RNA glycoLINC assembles a lower glycolytic metabolon to promote glycolysis. Mol Cell. 2022;82(3):542–54.

56. Didiasova M, Schaefer L, Wygrecka M. When place matters: shuttling of Enolase-1 Across Cellular compartments. Front Cell Dev Biol. 2019;7:61.

57. Nelson SM, Telfer EE, Anderson RA. The ageing ovary and uterus: new biological insights. Hum Reprod Update. 2013;19(1):67–83.

58. Wu J, Liu Y, Song Y, Wang L, Ai J, Li K. Aging conundrum: a perspective for ovarian aging. Front Endocrinol (Lausanne). 2022;13:952471.

59. Tu J, Chen Y, Li Z, Yang H, Chen H, Yu Z. Long non-coding RNAs in ovarian granulosa cells. J Ovarian Res. 2020;13(1):63.

60. Colella M, Cuomo D, Peluso T, Falanga I, Mallardo M, De Felice M, et al. Ovarian aging: role of Pituitary-Ovarian Axis hormones and ncRNAs in regulating ovarian mitochondrial activity. Front Endocrinol (Lausanne). 2021;12:791071.

61. Takeiwa T, Ikeda K, Horie-Inoue K, Inoue S. Mechanisms of apoptosis-related long non-coding RNAs in Ovarian Cancer. Front Cell Dev Biol. 2021;9:641963.

62. Tremblay PG, Sirard MA. Transcriptomic analysis of gene cascades involved in protein kinase A and C signaling in the SVOG line of human ovarian granulosa tumor cells†. Biol Reprod. 2017;96(4):855–65.

63. Chi JR, Yu ZH, Liu BW, Zhang D, Ge J, Yu Y et al. SNHG5 promotes breast cancer proliferation by sponging the miR-154-5p/PCNA Axis. Mol Ther Nucleic Acids. 2019;17:138–49.

64. Liu Y, Cheng G, Huang Z, Bao L, Liu J, Wang C, et al. Long noncoding RNA SNHG12 promotes tumour progression and sunitinib resistance by upregulating CDCA3 in renal cell carcinoma. Cell Death Dis. 2020;11(7):515.

65. Xu M, Chen X, Lin K, Zeng K, Liu X, Xu X, et al. lncRNA SNHG6 regulates EZH2 expression by sponging miR-26a/b and miR-214 in colorectal cancer. J Hematol Oncol. 2019;12(1):3.

Publisher's note